Original article

Nuclear Medicine Communications

Diagnostic value of ^{99m}Tc-ubiquicidin scintigraphy for osteomyelitis and comparisons with ^{99m}Tc-methylene diphosphonate scintigraphy and magnetic resonance imaging

Majid Assadi[a], Katayoun Vahdat[c], Iraj Nabipour[d], Mohammad Reza Sehhat[a], Fahimeh Hadavand[c], Hamid Javadi[e], Alireza Tavakoli[b], Jamshid Saberifard[a], Mohammad Reza Kalantarhormozi[d], Alireza Zakani[f] and Mohammad Eftekhari[f]

Objective **The discrimination of bacterial infections from sterile inflammatory processes is of great importance in the management of inflammation. Currently available techniques cannot decisively address this issue. In this respect, antimicrobial peptide ^{99m}Tc-ubiquicidin (UBI) 29–41 scans have been showing interesting results. The aim of this study was to determine the accuracy of ^{99m}Tc-UBI scan in the detection of osteomyelitis and to compare it with ^{99m}Tc-methylene diphosphonate scan and magnetic resonance imaging (MRI).**

Methods **Twenty patients (mean age = 48.90 years) with suspected osteomyelitis were included in this study. After evaluation of each patient through history taking, physical examination, appropriate laboratory tests, and other processes including bone probing, wound culture, and plain film radiography, MRIs, ^{99m}Tc-UBI scans, and ^{99m}Tc-methylene diphosphonate scans were performed. For quantitative analysis, the mean count of abnormal-to-normal (A/N) region was calculated for images acquired at 15, 30, 45, 60, 120, and 240 min to obtain the most favorable time for imaging.**

Results **In total, osteomyelitis was detected in the ^{99m}Tc-UBI scans of 17 patients, indicating 100% accuracy, compared with an accuracy of 90% for osteomyelitis detected in three-phase bone scans. The maximum mean A/N was observed at 15 min after intravenous injection (median: 1.91; interquartile range: 1.54–2.94). MRI was performed in 12 cases only with 75% accuracy. In addition, the A/N ratios for the ^{99m}Tc-UBI scans were not significantly different between patients with or without *Staphylococcus aureus* growth on wound cultures.**

Conclusion **For fast imaging with high accuracy, ^{99m}Tc-UBI 29–41 is a suitable choice for the detection of osteomyelitis. *Nucl Med Commun* 32:716–723 © 2011 Wolters Kluwer Health | Lippincott Williams & Wilkins.**

Nuclear Medicine Communications 2011, **32**:716–723

Keywords: antimicrobial peptides, infection, magnetic resonance imaging, osteomyelitis, ^{99m}Tc-methylene diphosphonate scan, ^{99m}Tc-ubiquicidin scan

[a]The Persian Gulf Nuclear Medicine Research Center, [b]Department of Orthopedic Surgery, Faculty of Medicine, Departments of [c]Infectious Diseases, [d]Endocrine and Metabolic Diseases, The Persian Gulf Tropical Medicine Research Center, Bushehr University of Medical Sciences, Bushehr, [e]Golestan Research Center of Gastroenterology and Hepatology (GRCGH), Golestan University of Medical Sciences (GUOMS), Gorgan and [f]Department of Nuclear Medicine, Imam Khomeini (Valiasr) Hospital, Faculty of Medicine, Tehran University of Medical Sciences, Tehran, Iran

Correspondence to Majid Assadi, MD, The Persian Gulf Nuclear Medicine Research Center, Bushehr University of Medical Sciences, Bushehr 3631, Iran
Tel: +98 771 2580169; fax: +98 771 2541828;
e-mail: assadipoya@yahoo.com; asadi@bpums.ac.ir

Received 7 February 2011 **Revised** 25 April 2011
Accepted 27 April 2011

Introduction

The timely and accurate clinical diagnosis of infectious diseases can be challenging, but is critical to the patient's outcome. The presently available radiopharmaceuticals are often incapable of determining between sterile inflammation and infection. Many pharmaceuticals labeled with different radioisotopes, such as immunoglobulins [1,2], liposomes labeled with ^{99m}Tc [3], the avidin–biotin system [4], antigranulocyte antibodies and antibody fragments, chemotactic peptides, cytokines, interleukins, platelet factor 4, and ciprofloxacin labeled with ^{99m}Tc [5] have been used, but an optimal agent has not yet been found. Thus, autologous leukocytes labeled with ^{111}In or ^{99m}Tc-hexamethylpropyleneamine oxime are still considered the gold standard despite the practical limitations of considerable time and labor for preparation and the necessity of a sterile environment [6]. The most promising choice is directly targeting infectious agents with radiolabeled antibiotics or antimicrobial peptides [7].

In this respect, a number of radiolabeled peptides have been assessed for the scintigraphic recognition of infections [8,9]. The most promising ones among them are ^{99m}Tc-labeled cationic antimicrobial peptides originating from ubiquicidin (UBI), which remarkably bind to microorganisms [10,11]. These radiolabeled antimicrobial peptides result in the rapid visualization of Gram-positive and Gram-negative bacterial infections [12] and fungi [10], with the least accumulation at sites of sterile inflammation [11]. Furthermore, ^{99m}Tc-UBI 29–41 has been used to monitor the effectiveness of treatment of experimental infections in animals [13]. Although results

0143-3636 © 2011 Wolters Kluwer Health | Lippincott Williams & Wilkins DOI: 10.1097/MNM.0b013e3283483fe4

from limited preclinical and pilot studies in patients are promising [14,15], this important agent is not currently available for routine clinical use. The aim of this study was to compare the sensitivity and specificity of ^{99m}Tc-labeled UBI scintigraphy with bone scans in the diagnosis of osteomyelitis. In addition, we had two other objectives: (a) whenever possible, compare this modality with magnetic resonance imaging (MRI) and (b) assess the feasibility of this radiotracer for routine practice.

Materials and methods

Participants

This study was conducted on 20 patients who were referred to our nuclear medicine department with clinical suspicion of osteomyelitis, due to diabetic foot ulcers, inflammation at the site of prosthesis, or bone fractures. The patients were recruited from a university hospital from 2008 to 2010. Before starting the antibiotic treatment, the patients first underwent ^{99m}Tc-UBI scanning, followed by three-phase ^{99m}Tc-methylene diphosphonate (MDP) bone scanning with a 4-day interval.

On the primary visit, wound culture and careful physical examination, including probing and, when possible, bone biopsy, were performed by infectious or orthopedic specialists and laboratory staff from the Department of Infectious Disease at our hospital.

The study complies with the Declaration of Helsinki and was approved by the Institutional Ethics Committee of Bushehr University of Medical Sciences; all patients provided written informed consent.

Imaging protocols

^{99m}Tc-ubiquicidin scintigraphy

Scans were performed using a dual-head ADAC camera, (ADAC Genesys, Malpitas, California, USA) equipped with a pair of low-energy, high-resolution collimators. Preparation of ^{99m}Tc-UBI entailed adding 740 MBq (20 mCi) ^{99m}Tc to vials of HYNIC-UBI 29–41 from a kit [14] (Radioisotope Division, Atomic Energy Organization of Iran) and incubating for 15 min at room temperature. The average radiochemical purity of ^{99m}Tc-HYNIC-UBI 29–41, produced by lyophilized kits, was more than 95%, congruent with a specific activity of 67.6 GBq/μmol, obtained by high-performance liquid chromatography, instant thin-layer chromatography, and solid-phase extraction. Immediately after intravenous (i.v.) injection of 740 MBq of ^{99m}Tc-UBI, dynamic imaging for 60 s for each frame up to 15 min was performed on the suspected infection area and the contralateral normal region as a nontarget area. Similarly, whole-body anterior and posterior projections followed by spot views of the region of interest (ROI) were also acquired at 15, 30, 45, 60, 120, and 240 min postinjection. An expert nuclear medicine specialist evaluated projections to optimize the quality of the images.

Quantitative analysis

Positive ^{99m}Tc-UBI scans were further analyzed by drawing manual ROIs over the suspected abnormal and contralateral normal bony sites. By selection of ROI analysis of the manipulation menu of the process menu in the ADAC software, the entire lesion was included in the region and mean counts per pixel in each region were measured. The mean uptake count ratios between abnormal and contralateral normal sites (A/N) were also obtained; these indices were acquired from the reference images.

^{99m}Tc-methylene diphosphonate scintigraphy

Bone scans were performed using 740 MBq (20 mCi) of ^{99m}Tc-MDP. The first phase of the bone scan consisted of a radionuclide angiogram, comprised of sequential images at 2–3 s per frame over the involved region of suspected osteomyelitis and the opposite presumed normal anatomic region. The flow phase was carried out for 60 s, followed by a blood-pool image at 180 s post i.v. injection of the radiopharmaceutical. Furthermore, 120 min post i.v. injection of the ^{99m}Tc-MDP (740 MBq), whole-body bone scintigraphy with multiple spot views was performed.

All the radionuclide images were read by two nuclear medicine physicians without knowledge of radiological and laboratory data.

In the interpretation of the ^{99m}Tc-UBI scan, there are four degrees; score 0 equals soft tissue; score 1, less than liver uptake; score 2 is more than or equal to liver uptake; and score 3 is more than or equal to the renal uptake [16]. Infection was considered based on scores of 2 or 3 on the ^{99m}Tc-UBI scan [16].

Osteomyelitis was determined based on a significant uptake of radiopharmaceutical in all three phases of ^{99m}Tc-MDP or an accumulation on the ^{99m}Tc-UBI scans as mentioned above (Figs 1 and 2). Remarkable radionuclide uptake on the ^{99m}Tc-MDP without significant uptake on the ^{99m}Tc-UBI scan was considered indicative of aseptic inflammation (Fig. 3).

Magnetic resonance imaging

MRI was performed with 1.5-T Signal imager (General Electric, Milwaukee, Wisconsin, USA) with three spin-echo pulse sequences emphasizing T1-weighted, T2-weighted, and fluid-attenuated inversion recovery-weighted information. The scans and MRI were performed within a 3-day interval. Plain film radiography (PFR) and MRI images were interpreted separately by two expert radiologists without awareness of the results of scintigraphy and laboratory tests. On unenhanced images, the MRI criteria for the presence of osteomyelitis were diminished signal intensity on the T1-weighted sequences and increased signal intensity on T2-weighted sequences within the bone

Fig. 1

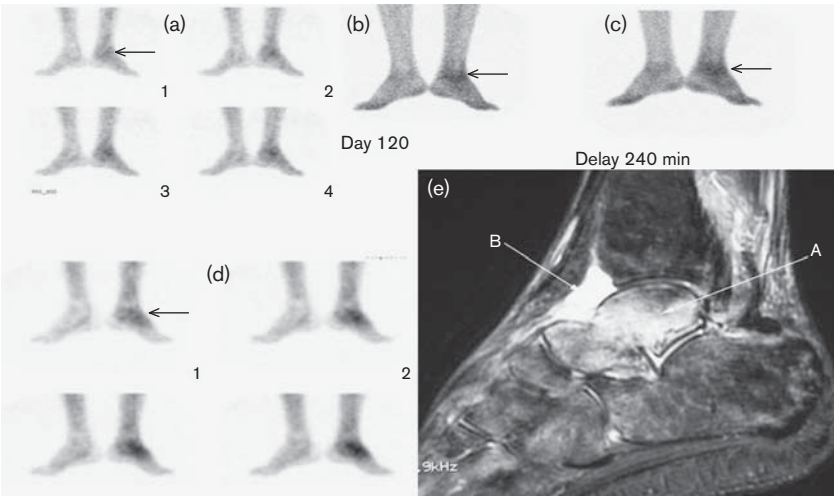

There is a significant activity in the left ankle in the early views (1–45 min) of ^{99m}Tc-ubiquicidin scintigraphy of a 44-year-old thallasemic male patient (patient number 4), which persists over the course of the study (up to 240 min; a–c). The whole-body bone scan also shows osteomyelitis in the same region (d). In addition, osteomyelitis is evident in the tarsal bones as bone marrow hyperintensity on the fat-suppressed T2-weighted magnetic resonance image (arrow a). There is also a small amount of joint effusion (arrow b), which could be suggestive of concomitant septic arthritis (e). *Staphylococcus aureus* was isolated from the wound culture.

Fig. 2

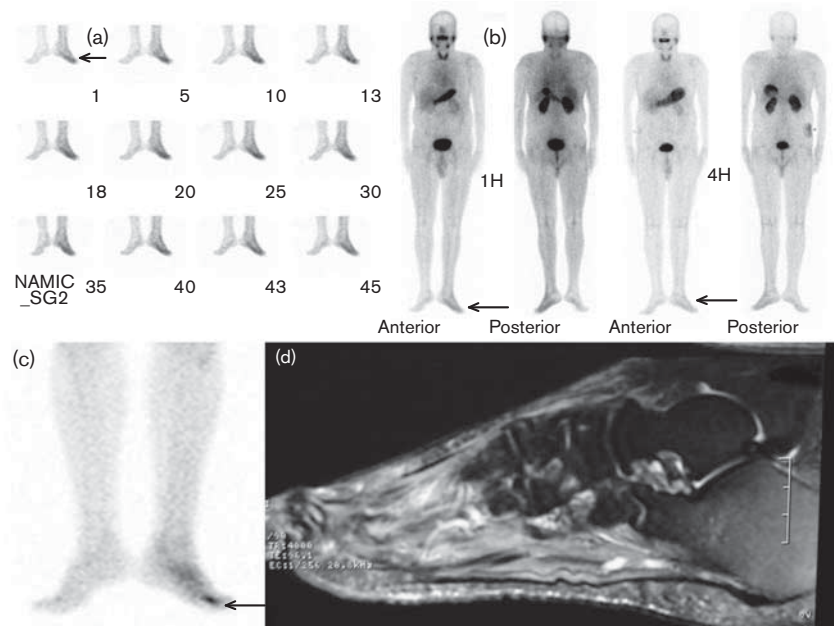

There is significant activity in the left metatarsal and left first toe bones in the early views (1–45 min) of ^{99m}Tc-ubiquicidin scintigraphy of a 52-year-old diabetic male patient (patient number 7), which persists over the course of the study (up to 240 min; a and b). The three-phase body bone scan also shows osteomyelitis in the same region (c). In contrast, the fat-suppressed T2-weighted magnetic resonance image does not indicate osteomyelitis (d). *Pseudomonas aeruginosa* was isolated from the wound culture.

marrow [17]. After contrast administration, focal abnormal bone marrow enhancement on fat-suppressed T1-weighted images was considered as osteomyelitis [17]. When visible radiographically on PFR, focal bone rarefaction, diminished bone density, periostitis, bone erosion, or destruction were considered as osteomyelitis.

Gold standard

The final diagnosis was according to the consensus of clinicians according to clinical presentation, histopathologic examinations, wound culture, probing, response to antibiotic therapy, laboratory tests, and clinical follow-up. The clinicians were blinded for all imaging results.

Statistical analysis

The distribution of variables was assessed using probability plots and the Shapiro–Wilk test, and they were not fit to a Gaussian distribution. The Mann–Whitney *U*-test was applied for the quantitative comparison of A/N ratios between patients with and without *Staphylococcus aureus* (*S. aureus*) in their wound cultures. The Wilcoxon test was used for the comparison of A/N ratios in different times. The images were categorized as true positive (TP), true negative (TN), false positive (FP), or false negative (FN). Thereafter, the statistical parameters were determined as follows: specificity [TN/(TN + FP)], sensitivity [TP/(TP + FN)], PPV [TP/(TP + FP)], NPV [TN/(TN + FN)], and accuracy [(TP + TN)/(TP + TN + FN + FP)].

Fig. 3

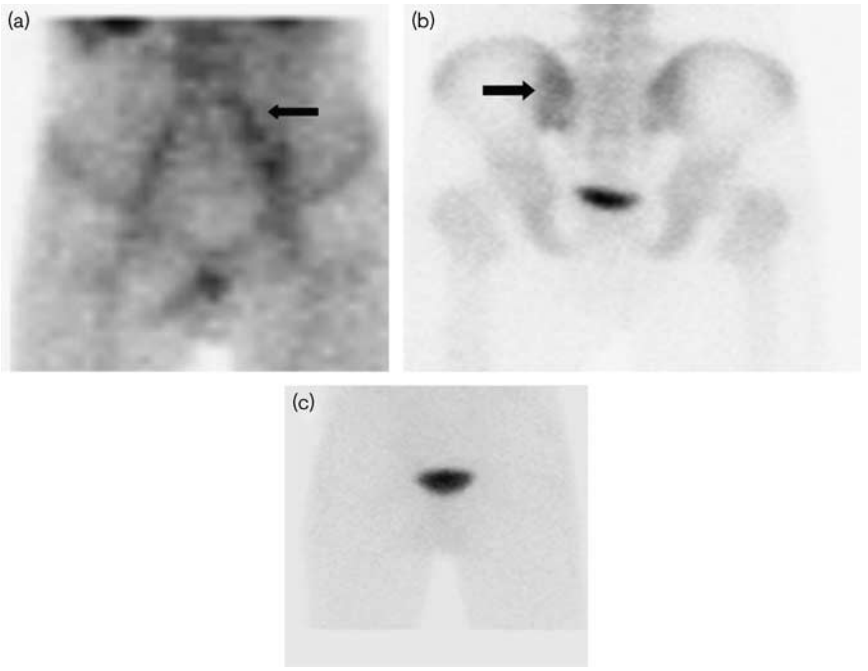

There is significant uptake of ^{99m}Tc-methylene diphosphonate in the left sacroiliac joint of a 20-year-old thallasemic male patient (patient number 1) in bone scintigraphy (a and b) without significant uptake in the ^{99m}Tc-ubiquicidin scan (c), indicating aseptic inflammation.

Table 1 Total outcomes of the scintigraphy studies

Patient number	Ulcer location	History	PFR	MRI	Three-phase ^{99m}Tc-MDP	^{99m}Tc-UBI	Gold standard	Final diagnosis
1	Sacroiliac joint	Thalassemia	TN	TN	FP	TN	CP, CF, RTT	No infection
2	Left ankle	DM	TN	TN	TN	TN	CP, CF, probing, RTT	No infection
3	Right medial malleolus	Fracture	TP	TP	TP	TP	WC, biopsy	Osteomyelitis
4	Right tibia, Right Femur	Fracture	FN	FN	TP	TP	WC, biopsy, probing	Osteomyelitis
5	Left ankle	Thalassemia	TP	TP	TP	TP	WC, biopsy	Osteomyelitis
6	Left calcaneus	DM	FN	TP	TP	TP	WC, biopsy, probing	Osteomyelitis
7	Left metatarsi, left first toe	DM	FN	FN	TP	TP	WC, probing, biopsy	Osteomyelitis
8	Left calcaneus	DM	TP	NA	TP	TP	CP, CF, probing	Osteomyelitis
9	Right metatarsi	DM	TP	NA	TP	TP	CP, CF, WC, probing	Osteomyelitis
10	Right calcaneus	DM	TP	TP	TP	TP	WC, probing, RTT	Osteomyelitis
11	Left metatarsi	DM	FN	TP	TP	TP	WC, probing, RTT	Osteomyelitis
12	Left tibia	Fracture, prosthesis	TP	NA	TP	TP	CP, biopsy	Osteomyelitis
13	Both tibiae	IVDU	TP	TP	TP	TP	CP, WC	Osteomyelitis
14	Sacroiliac joint	Bedsore	FN	NA	TP	TP	WC, probing, biopsy	Osteomyelitis
15	Right metatarsi	DM	FN	NA	TP	TP	CP, CF, WC, probing	Osteomyelitis
16	Left tibia, left fibula	Fracture	FN	FN	TP	TP	WC, biopsy, probing	Osteomyelitis
17	Left metatarsi	DM	TN	TN	FP	TN	Probing, biopsy	No infection
18	Right tibia	DM	FN	NA	TP	TP	WC, probing, biopsy	Osteomyelitis
19	Left tibia	Fracture, prosthesis	FN	NA	TP	TP	WC, biopsy	Osteomyelitis
20	Right tibia	DM	TP	NA	TP	TP	WC, biopsy	Osteomyelitis

CF, clinical follow-up; CP, clinical presentation; FN, false negative; FP, false positive; MDP, methylene diphosphonate; MRI, magnetic resonance imaging; OS, orthopedic surgery; PFR, plain film radiography; RTT, response to treatment; TN, true negative; TP, true positive; UBI, ubiquicidin; WC, wound culture.

A *P* value of less than 0.05 was considered to be statistically significant. Statistical analysis was conducted using an IBM computer and PASW software, version 18.0 (SPSS, Inc., Chicago, Illinois, USA).

Results

The study included 12 men and eight women (mean age, 48.90 ± 15.37 years; range, 20–69 years). Eleven patients had diabetes mellitus; five patients had fractures and/or prostheses; two patients had thalassemia; one patient had a bedsore; and one had a history of drug abuse. From a total of 20 patients, 17 cases had osteomyelitis and three cases had aseptic inflammation (Table 1).

None of the patients had any adverse reactions after the i.v. injection of ^{99m}Tc-HYNIC-UBI 29–41, and no side effects were reported up to 14 days after the administration.

There was a complete agreement between specialists in interpretations of scans, PFR, and MRI in this study.

For the diagnosis of osteomyelitis, ^{99m}Tc-UBI scans showed 100% (17/17) sensitivity and specificity (3/3). ^{99m}Tc-MDP scans showed an excellent sensitivity for the diagnosis of osteomyelitis, but the specificity was significantly compromised [100% (17/17) and 33% (1/3), respectively]. Osteomyelitis could not be differentiated from aseptic inflammation (Table 2). Even in early views, ^{99m}Tc-UBI scans revealed rapid tracer distribution with higher activity at the site of infection than on the contralateral healthy side (Fig. 2a).

Furthermore, for quantitative analysis, A/Ns were calculated for images acquired at 15, 30, 45, 60, 120, and 240 min to get the most favorable imaging time. The maximum A/N ratio was observed at 15 min after i.v. injection (median: 1.91; interquartile range: 1.54–2.94). In addition, the A/N ratio at 30 min was 1.84, 1.65–2.57; 45 min, 1.82, 1.70–2.64; 60 min, 1.81, 1.70–2.28; 120 min, 1.78, 1.45–2.06; and at 240 min, it was 1.53, 1.36–1.89. There are significant differences among A/N ratios of the early views in comparison with delayed views at 240 min (P value < 0.05). The A/Ns for all patients at the different times are compared in Fig. 4.

Similarly, wound culture was performed on 15 patients. Bacterial growth was reported in 11 cases: Gram-negative bacterial infection was found in three cases and mixed or pure *S. aureus* was isolated from the eight remaining participants. Specifically, *S. aureus*, *Escherichia coli* (*E. coli*), *Klebsiella pneumonia*, *Pseudomonas aeruginosa*, *Staphylococcus epidermis*, and *Acinetobacter* were reported. In comparisons of the patients according to the presence or absence of *S. aureus* infection in their wound cultures (Table 3), the A/N indices were not significantly different at early and delayed views over the course of the study on ^{99m}Tc-UBI scans ($P > 0.05$).

PFR had 47% (8/17) sensitivity and 100% (3/3) specificity for osteomyelitis detection as diagnosed by the gold standard. On account of metallic prostheses or, in some cases, the patient's refusal, MRI was taken in only 12 cases, resulting in 66.66% (6/9) sensitivity and 100% (3/3) specificity and three FN cases (Fig. 2). In 11 diabetic patients, MRI also resulted in one FN case, whereas the ^{99m}Tc-UBI scan was accurate in all of them.

Statistical analysis revealed an accuracy of 100% (20/20) for ^{99m}Tc-UBI scintigraphy, 90% (18/20) for ^{99m}Tc-MDP scintigraphy, 75% (9/12) for MRI, and 55% (11/20) for radiograph (Table 2).

Table 2 The statistical values of different modalities in detection of osteomyelitis

	PFR	MRI (12 case)	Three-phase ^{99m}Tc-MDP	^{99m}Tc-UBI
Sensitivity (%)	47 (8/17)	66.66 (6/9)	100 (17/17)	100 (17/17)
Specificity (%)	100 (3/3)	100 (3/3)	33 (1/3)	100 (3/3)
PPV (%)	100 (8/8)	100 (6/6)	89 (17/19)	100 (17/17)
NPV (%)	25 (3/12)	50 (3/6)	100 (1/1)	100 (3/3)
Accuracy (%)	55 (11/20)	75 (9/12)	90 (18/20)	100 (20/20)

MDP, methylene diphosphonate; MRI, magnetic resonance imaging; NPV, negative predictive value; PFR, plain film radiography; PPV, positive predictive value; UBI, ubiquicidin.

Fig. 4

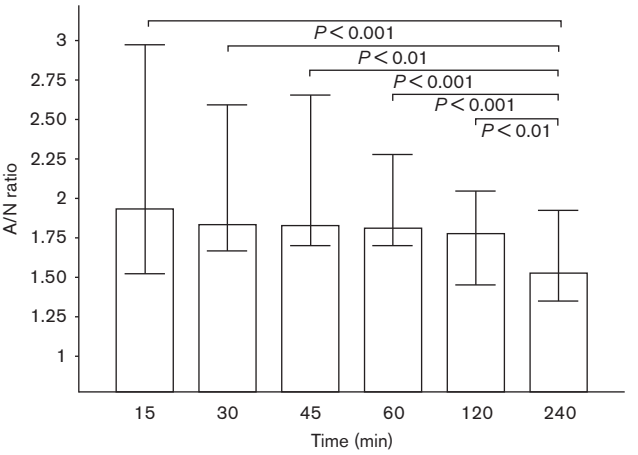

The median and interquartile ranges of the abnormal-to-normal (A/N) ratios in different time images during ^{99m}Tc-ubiquicidin scintigraphy. There are significant differences among A/N ratios of the early views in comparison with delayed view at 240 min ($P<0.05$).

Table 3 The comparison of abnormal-to-normal ratios between patients with and without *Staphylococcus aureus* in their wound cultures during ^{99m}Tc-ubiquicidin scintigraphy

Postinjection time (min)	*Staphylococcus aureus*	Non-*Staphylococcus aureus*	*P* value
15	1.80 (1.64–3.23)	1.93 (1.43–2.33)	0.83
30	1.84 (1.68–2.57)	2.00 (1.28–2.29)	0.68
45	1.77 (1.70–2.55)	2.00 (1.28–2.40)	0.83
60	1.78 (1.70–2.32)	2.00 (1.24–2.22)	0.87
120	1.78 (1.40–1.86)	1.60 (1.20–2.10)	0.68
240	1.51 (1.33–1.58)	1.44 (1.30–1.96)	0.75

The data were expressed as median, interquartile range.

Discussion

Anatomical imaging modalities are often inappropriate for the early detection of infection because such techniques are focused only on morphological changes [10,18], whereas nuclear imaging can easily detect an inflammatory process because it is based on functional processes, which are morphologically indistinguishable [19]. In view of this, infection is usually accompanied by inflammation; it is much more valuable to make a distinction between infection and inflammation. In the quest for this distinction, a broad range of radiopharmaceuticals has been suggested. Radiolabeled leukocytes and gallium-67-citrate are the most frequently applied radiopharmaceuticals [20]. However, there is continuous investigation into new radiopharmaceuticals that allow fast and precise detection of lesions without the drawbacks of the presently used radiotracers that require arduous and sophisticated preparation and present contamination risks [21]. Radiolabeled monoclonal antibodies in opposition to outside antigens of granulocytes have the risk of induction of human antimouse antibodies [22]. In addition, antibody fragments, interleukins, and platelet factor 4 have certain limitations [5]. Cytokines and chemotactic peptides are immunogenic and cytotoxic [23]. There are conflicting results regarding radiolabeled ciprofloxacin against microorganisms responsible for infection [24,25]. Although positron emission tomography (PET)-computed tomography using ^{18}F-fluorodeoxyglucose (FDG) may be promising for imaging bone infections [26–28], the impact of elevated serum glucose levels, present mainly in diabetic patients, on PET sensitivity is a controversial issue [29]. In addition, its high charge and limited accessibility hinder its widespread use in the detection of osteomyelitis.

However, from the earliest gallium-67-citrate imaging to the latest ^{18}F-FDG PET imaging, the main question has not been satisfactorily answered [15,18]. In all radiopharmaceuticals, antimicrobial peptides that attach directly to bacteria are preferred over pharmaceuticals that have an indirect approach (such as binding to leukocytes or antigranulocyte antibodies) [22]. Among the peptides, ^{99m}Tc-UBI 29–41 scans have shown the most promising results for differentiation between infection and inflammation in animal models [11,12,30] and also in limited human studies [22].

In this study, the sensitivity, specificity, and overall diagnostic accuracy of ^{99m}Tc-UBI 29–41 scans for the detection of osteomyelitis were 100%. To our knowledge, this is the first clinical study to compare ^{99m}Tc-UBI scan with conventional modalities in the detection of osteomyelitis in humans. In other studies conducted by Melendez-Alafort *et al.* [31] and Becker and Meller [18], 100% sensitivity and specificity were also shown, whereas in another study by Akhtar *et al.* [22], the sensitivity and specificity values were 100 and 80%, respectively. In a small study, in seven patients with the same method of preparation and labeling, ^{99m}Tc-UBI also showed 100% accuracy in osteomyelitis detection [14]. Recently, in a study of 196 patients with fever of unknown origin, specificity for discrimination between sterile inflammation and infection was 95.35%, sensitivity was 97.52%, and accuracy was 96.62% [15]. In addition, another study showed that the ^{99m}Tc-UBI 29–41 scan is a promising agent for the specific detection of infections in humans because of its high sensitivity (96.3%), specificity (94.1%), and accuracy (95.3%) [32].

Therefore, ^{99m}Tc UBI 29–41, without accumulation in sterile inflammation and lack of immunological adverse effects, may be considered an alternative for leukocyte labeling, which is still used as the gold standard for infection detection in nuclear medicine and it is applicable in leukopenic patients. In another study, it was shown that ^{99m}Tc-UBI (29–41) accumulation directly draws parallels with the number of viable bacteria and it can be used for monitoring efficacy and duration of antibiotic treatment [16].

In this study, the maximum contrast (A/N ratio) was obtained 15 min after ^{99m}Tc-UBI administrations, as previously mentioned [14,22]. These data may suggest a first pass-like distribution with strong avidity of the tracer in the direction of its targets, facilitating image interpretation to distinguish infection as early as 15 min postinjection. In this (Fig. 2b) and previous human studies, ^{99m}Tc-UBI 29–41 scans expressed rapid concentration to the target region and fast renal clearance with negligible liver uptake and hepatobiliary excretion [14,22,31].

Akhtar *et al.* [7] revealed that ^{99m}Tc-UBI 29–41 had less avidity at sites infected with *E. coli* than *S. aureus*. They suggested that the lower accumulation with *E. coli* compared with *S. aureus* may be due to either a lower virulence of the bacterial strain or a diminished affinity of the peptide for the bacterial membranes. In contrast, our study did not show any significant difference between those sites infected with *S. aureus* and those not infected. Multiple factors may be responsible for this result, such as not using a wide range of culture media for growth of anaerobic bacteria and fungi, and the fact that most of the wound cultures in this investigation contained mixed growth.

On the basis of these observations, the investigators suggested that ^{99m}Tc-UBI 29–41 could be used for the detection of infections in humans. Meléndez-Alafort *et al.* [31] evaluated the use of ^{99m}Tc-UBI 29–41 scans as an infection imaging agent in six children suspected of having bone infection, and compared with ^{67}Ga scanning, concluded that ^{99m}Tc-UBI 29–41 could be used for the detection of infections in humans [31]. In a similar study in 18 adult [22] patients who participated in the trial, 14 were positive for infection as determined with the use of ^{99m}Tc-UBI 29–41 scans. The investigators concluded that ^{99m}Tc-UBI 29–41 is an effective agent for the imaging of infection [22].

In general, the diagnosis of musculoskeletal infection and osteomyelitis can be clinically challenging in practice. Infected foot ulcers in the diabetic patient comprise up to 90% of pedal osteomyelitis cases [33]. Devillers *et al.* [34] studied 56 diabetic foot ulcers in 40 patients, and reported that the accuracy of radiography, ^{99m}Tc-MDP, and ^{99m}Tc-hexamethylpropyleneamine oxime-conjugated leukocyte scintigraphy was 69.6, 62.5, and 92.9%, respectively. They suggested that leukocyte-labeling scintigraphy can be considered the gold standard technique for the identification of osteomyelitis in the diabetic foot. Although it is accurate, leukocyte-labeling scintigraphy accompanying bone marrow scan is doomed due to inaccessibility, labor intensity, and the risk of contamination [35]. In addition, bone scan can be a sensitive method for the diagnosis of osteomyelitis. However, it does not discriminate diabetic osteomyelitis from other osteoarthropathic conditions due to higher bone turnover in both conditions [36].

Moreover, based on the literature, MRI can efficiently discriminate soft tissue infection from bone involvement. It can also effectively detect the development of infection in anterior parts of the bone. However, its efficacy is dramatically compromised at the mid foot and hind foot [33,37–39]. Despite its high sensitivity, MRI application for the recognition of osteomyelitis in the diabetic foot is compromised due to lower specificity related to Charcot neuropathic osteoarthropathy. In addition, if there is inflammatory hyperemia, the diagnostic accuracy is further hampered to 40–50% [40]. In a recent study by Bae *et al.* [41] in 35 cases, three-phase bone scans showed a sensitivity of 83% (5/6), specificity of 93% (27/29), positive predictive value (PPV) of 71% (5/7), and negative predictive value (NPV) of 96% (18/27) in the diagnosis of osteomyelitis. MRI showed sensitivity of 83% (5/6), specificity of 93% (27/29), PPV of 71% (5/7), and NPV of 89% (24/27) in the diagnosis of osteomyelitis. In another study of 110 consecutive patients with diabetic foot, FDG-PET had sensitivity, specificity, PPV, NPV, and accuracy of 81, 93, 78, 94, and 90%, respectively. MRI soundly assessed osteomyelitis in 20 of 22 patients and properly excluded it in 56 of 72 patients, with sensitivity, specificity, PPV, NPV, and accuracy of 91, 78, 56, 97, and 81%, respectively. PFR also had sensitivity, specificity, PPV, NPV, and accuracy of 63, 87, 60, 88, and 81%, respectively [28].

In the participants in our study, MRI accuracy was 75%; we had three FN results, which may have been due to our specific population. This study shows that ^{99m}Tc-UBI imaging could be a promising modality in diabetic patients and cases in which MRI is contraindicated. However, in a meta-analysis of 16 studies, MRI was shown to be superior to radiographs, white blood cell scanning, and three-phase bone scans. Therefore, we recommend further evaluation of our comment in a larger study [42].

Although our study demonstrates good insight into using ^{99m}Tc-UBI compared with ^{99m}Tc-MDP and MRI in osteomyelitis assessment, it should be noted that it has some shortcomings. The major limitations are the relatively small sample size with different underlying problems and the absence of bone biopsy in all patients as a gold standard test, both of which may have influenced the results of this study. However, we did consider compound clinical presentation, histopathologic examinations, and follow-up evaluation to mitigate this deficiency. Our results should be validated in a larger and well-designed study.

Conclusion

In summary, ^{99m}Tc-UBI 29–41 scans can be applied to detect bone involvement in infection with excellent sensitivity and specificity in distinguishing between infection and inflammation in early views. These data also showed that the use of ^{99m}Tc-UBI in osteomyelitis studies might lead to images comparable with MRI; however, further studies are recommended.

Acknowledgements

This study was achieved with the sponsorship of Bushehr University of Medical Sciences (grant no. 546). The authors thank colleagues at our institutes especially S.R. Mosavi, M. Kassaian, and Kh. Golzari for their technical help and assistance with data acquisition.

The authors declare that they have no conflicts of interest.

References

1 Calame W, Welling M, Feitsma HI, Ensing GJ, Pauwels EK. Improved detection of a staphylococcal infection by monomeric and protein A-purified polyclonal human immunoglobulin. *Eur J Nucl Med* 1993; **20**:490–494.
2 Welling M, Feitsma HI, Calame W, Pauwels EK. Localization of a bacterial infection with ^{99}Tc^{m}-labelled human IgG: further improvement with enriched IgG subclass preparations. *Nucl Med Commun* 1997; **18**:1057–1064.
3 Dams ET, Oyen WJ, Boerman OC, Storm G, Laverman P, Kok PJ, *et al.* ^{99m}Tc-PEG liposomes for the scintigraphic detection of infection and inflammation: clinical evaluation. *J Nucl Med* 2000; **41**:622–630.
4 Hnatowich DJ, Virzi F, Rusckowski M. Investigations of avidin and biotin for imaging applications. *J Nucl Med* 1987; **28**:1294–1302.
5 Britton KE, Vinjamuri S, Hall AV, Solanki K, Siraj QH, Bomanji J, Das S. Clinical evaluation of technetium-99m infecton for the localisation of bacterial infection. *Eur J Nucl Med* 1997; **24**:553–556.
6 Weon YC, Yang SO, Choi YY, Shin JW, Ryu JS, Shin MJ, *et al.* Use of Tc-99m HMPAO leukocyte scans to evaluate bone infection: incremental value of additional SPECT images. *Clin Nucl Med* 2000; **25**:519–526.
7 Akhtar MS, Iqbal J, Khan MA, Irfanullah J, Jehangir M, Khan B, *et al.* ^{99m}Tc-labeled antimicrobial peptide ubiquicidin (29–41) accumulates less in Escherichia coli infection than in Staphlococcus aureus infection. *J Nucl Med* 2004; **45**:849–856.
8 Signore A, Annovazzi A, Chianelli M, Corsetti F, Van de Wiele C, Watherhouse RN. Peptide radiopharmaceuticals for diagnosis and therapy. *Eur J Nucl Med* 2001; **28**:1555–1565.
9 Welling MM, Visentin R, Feitsma HI, Lupetti A, Pauwels EK, Nibbering PH. Infection detection in mice using ^{99m}Tc-labeled HYNIC and N2S2 chelate conjugated to the antimicrobial peptide UBI 29–41. *Nucl Med Biol* 2004; **31**:503–509.

10 Lupetti A, Welling MM, Pauwels EK, Nibbering PH. Radiolabelled antimicrobial peptides for infection detection. *Lancet Infect Dis* 2003; **3**:223–229.
11 Welling MM, Lupetti A, Balter HS, Lanzzeri S, Souto B, Rey AM, *et al.* ^{99m}Tc-labeled antimicrobial peptides for detection of bacterial and Candida albicans infections. *J Nucl Med* 2001; **42**:788–794.
12 Welling MM, Paulusma-Annema A, Balter HS, Pauwels EK, Nibbering PH. Technetium-99m labelled antimicrobial peptides discriminate between bacterial infections and sterile inflammations. *Eur J Nucl Med* 2000; **27**:292–301.
13 Nibbering PH, Welling MM, Paulusma-Annema A, Brouwer CP, Lupetti A, Pauwels EK. ^{99m}Tc-Labeled UBI 29–41 peptide for monitoring the efficacy of antibacterial agents in mice infected with *Staphylococcus aureus*. *J Nucl Med* 2004; **45**:321–326.
14 Gandomkar M, Najafi R, Shafiei M, Mazidi M, Goudarzi M, Mirfallah SH, *et al.* Clinical evaluation of antimicrobial peptide [(99m)Tc/tricine/HYNIC(0)] ubiquicidin 29–41 as a human-specific infection imaging agent. *Nucl Med Biol* 2009; **36**:199–205.
15 Sepulveda-Mendez J, de Murphy CA, Rojas-Bautista JC, Pedraza-Lopez M. Specificity of ^{99m}Tc-UBI for detecting infection foci in patients with fever in study. *Nucl Med Commun* 2010; **31**:889–895.
16 Akhtar MS, Khan ME, Khan B, Irfanullah J, Afzal MS, Khan MA, *et al.* An imaging analysis of (99m)Tc-UBI (29–41) uptake in *S. aureus* infected thighs of rabbits on ciprofloxacin treatment. *Eur J Nucl Med Mol Imaging* 2008; **35**:1056–1064.
17 Averill LW, Hernandez A, Gonzalez L, Pena AH, Jaramillo D. Diagnosis of osteomyelitis in children: utility of fat-suppressed contrast-enhanced MRI. *AJR Am J Roentgenol* 2009; **192**:1232–1238.
18 Becker W, Meller J. The role of nuclear medicine in infection and inflammation. *Lancet Infect Dis* 2001; **1**:326–333.
19 Rennen HJ, Boerman OC, Oyen WJ, Corstens FH. Imaging infection/inflammation in the new millennium. *Eur J Nucl Med* 2001; **28**:241–252.
20 Knight LC. Non-oncologic applications of radiolabeled peptides in nuclear medicine. *Q J Nucl Med* 2003; **47**:279–291.
21 Weiner RE, Thakur ML. Radiolabeled peptides in diagnosis and therapy. *Semin Nucl Med* 2001; **31**:296–311.
22 Akhtar MS, Qaisar A, Irfanullah J, Iqbal J, Khan B, Jehangir M, *et al.* Antimicrobial peptide ^{99m}Tc-ubiquicidin 29–41 as human infection-imaging agent: clinical trial. *J Nucl Med* 2005; **46**:567–573.
23 Fischman AJ, Rauh D, Solomon H, Babich JW, Tompkins RG, Kroon D, *et al.* In vivo bioactivity and biodistribution of chemotactic peptide analogs in nonhuman primates. *J Nucl Med* 1993; **34**:2130–2134.
24 Vinjamuri S, Hall AV, Solanki KK, Bomanji J, Siraj Q, O'Shaughnessy E, *et al.* Comparison of ^{99m}Tc infection imaging with radiolabelled white-cell imaging in the evaluation of bacterial infection. *Lancet* 1996; **347**:233–235.
25 Larikka MJ, Ahonen AK, Niemela O, Junila JA, Hämäläinen MM, Britton K, *et al.* Comparison of ^{99m}Tc ciprofloxacin, ^{99m}Tc white blood cell and three-phase bone imaging in the diagnosis of hip prosthesis infections: improved diagnostic accuracy with extended imaging time. *Nucl Med Commun* 2002; **23**:655–661.
26 Basu S, Chryssikos T, Moghadam-Kia S, Zhuang H, Torigian DA, Alavi A. Positron emission tomography as a diagnostic tool in infection: present role and future possibilities. *Semin Nucl Med* 2009; **39**:36–51.
27 Keidar Z, Militianu D, Melamed E, Bar-Shalom R, Israel O. The diabetic foot: initial experience with ^{18}F-FDG PET/CT. *J Nucl Med* 2005; **46**:444–449.
28 Nawaz A, Torigian DA, Siegelman ES, Basu S, Chryssikos T, Alavi A. Diagnostic performance of FDG-PET, MRI, and plain film radiography (PFR) for the diagnosis of osteomyelitis in the diabetic foot. *Mol Imaging Biol* 2010; **12**:335–342.
29 Zhuang HM, Cortes-Blanco A, Pourdehnad M, Adam LE, Yamamoto AJ, Martinez-Lázaro R, *et al.* Do high glucose levels have differential effect on FDG uptake in inflammatory and malignant disorders? *Nucl Med Commun* 2001; **22**:1123–1128.
30 Sarda-Mantel L, Saleh-Mghir A, Welling MM, Meulemans A, Vrigneaud JM, Raguin O, *et al.* Evaluation of ^{99m}Tc-UBI 29–41 scintigraphy for specific detection of experimental *Staphylococcus aureus* prosthetic joint infections. *Eur J Nucl Med Mol Imaging* 2007; **34**:1302–1309.
31 Melendez-Alafort L, Rodriguez-Cortes J, Ferro-Flores G, Arteaga De Murphy C, Herrera-Rodríguez R, Mitsoura E, *et al.* Biokinetics of (99m)Tc-UBI 29–41 in humans. *Nucl Med Biol* 2004; **31**:373–379.
32 Arteaga de Murphy C, Gemmel F, Balter J. Clinical trial of specific imaging of infections. *Nucl Med Commun* 2010; **31**:726–733.
33 Palestro CJ, Love C. Nuclear medicine and diabetic foot infections. *Semin Nucl Med* 2009; **39**:52–65.
34 Devillers A, Moisan A, Hennion F, Garin E, Poirier JY, Bourguet P. Contribution of technetium-99m hexamethylpropylene amine oxime labelled leucocyte scintigraphy to the diagnosis of diabetic foot infection. *Eur J Nucl Med* 1998; **25**:132–138.
35 Dinh MT, Abad CL, Safdar N. Diagnostic accuracy of the physical examination and imaging tests for osteomyelitis underlying diabetic foot ulcers: meta-analysis. *Clin Infect Dis* 2008; **47**:519–527.
36 Seabold JE, Flickinger FW, Kao SC, Gleason TJ, Kahn D, Nepola JV, Marsh JL. Indium-111-leukocyte/technetium-99m-MDP bone and magnetic resonance imaging: difficulty of diagnosing osteomyelitis in patients with neuropathic osteoarthropathy. *J Nucl Med* 1990; **31**:549–556.
37 Hovi I. Complicated bone and soft-tissue infections: imaging with 0.1T MR and ^{99m}Tc-HMPAO-labeled leukocytes. *Acta Radiol* 1996; **37**:870–876.
38 Marcus CD, Ladam-Marcus VJ, Leone J, Malgrange D, Bonnet-Gausserand FM, Menanteau BP. MR imaging of osteomyelitis and neuropathic osteoarthropathy in the feet of diabetics. *Radiographics* 1996; **16**:1337–1348.
39 Palestro CJ, Love C, Miller TT. Infection and musculoskeletal conditions: imaging of musculoskeletal infections. *Best Pract Res Clin Rheumatol* 2006; **20**:1197–1218.
40 Rozzanigo U, Tagliani A, Vittorini E, Pacchioni R, Brivio LR, Caudana R. Role of magnetic resonance imaging in the evaluation of diabetic foot with suspected osteomyelitis. *Radiol Med* 2009; **114**:121–132.
41 Bae KUK, Kim SH, Oo JH, Sohn HS, Chung SK. Comparison between 3-phase bone scan and MRI in diagnosis of osteomyelitis. *J Nucl Med* 2010; **51** (**Suppl 2**):1653.
42 Kapoor A, Page S, Lavalley M, Gale DR, Felson DT. Magnetic resonance imaging for diagnosing foot osteomyelitis: a meta-analysis. *Arch Intern Med* 2007; **167**:125–132.